RETRIEVING PHOTOMETRIC PROPERTIES OF APOLLO 16 LANDING SITE USING TMC ONBOARD CHANDRAYAAN-2: PROSPECTS. *Rohit Nagori and A.S. Arya, Space Applications Centre, Indian Space Research Organisation (ISRO), Ahmedabad-380015, India. (*rohitnagori@sac.isro.gov.in).

Introduction: Retrieving photometric properties of Lunar surface may reveal a lot about the physical properties of the surface material, their scattering characteristics, etc. The parameters derived through physical models such as Hapke's form an important part of radiative transfer models and their variation within the surface may indicate difference in material properties [1][2][3]. Terrain Mapping Camera (TMC) -2 onboard Chandrayaan-2 is a panchromatic imaging camera with spatial resolution of 5m and stereo imaging capability, i.e., it images in three views of Fore, Nadir and Aft (+25°, 0°, -25°) and have identical specifications in comparison to TMC-1 [4]. In this study, using multi-view images acquired by TMC-1 over Apollo 16 region, a data requirement assessment has been made in order to ensure nearly uniform phase angle range for photometric parameters retrieval using physical model. Further, variation of Lommel Seeliger (LS) corrected radiance factor was also seen with respect to phase angles for a selected region in sample TMC-2 image highlighting the similar process to be applied for other available datasets.

Pre-Investment Study: TMC-1 image acquired on 01-08-2009 was considered for study. Dataset contained radiance images for all three views along with orthorectified Nadir image, Digital Elevation Model (DEM) image and files containing latitude-longitude and sun parameters information. Region around the Apollo 16 landing site (8.973 ºS, 15.498 ºE) was considered (Fig. 1) and viewing zenith and azimuthal angles were generated on per-pixel basis using ancillary information and mathematical formulations for all three views. Assuming the viewing geometry fixed, around 15 sub-solar points along the Lunar equator were considered in order to generate Sun incidence zenith and azimuthal angle images. Images are generated for all three views such that the Sun zenith angle values at the central pixel of the selected region are at an interval of 10 degrees with associated azimuthal angles (assuming that the variation in Sun incidence angle for aft and fore imaging of same region is negligible). Using the DEM image provided with dataset, slope and aspect images were generated which were then used to generate topographically corrected incidence and viewing' zenith and azimuthal angles on per-pixel basis. Subsequently, phase angle images were generated. Geological Map by USGS [5] near Apollo 16 landing site was considered and a demarcation was observed between Plains unit and Basin Undivided unit (Fig. 1). Same demarcation was observed in the DEM image provided with TMC dataset (Fig. 2). In order to consider similar material unit and advantage of local topography in generating variety of phase angles, Basin Undivided unit was marked and considered (Fig. 2). Further, histograms were generated for various combinations of set of phase angle images' values. This was done in order to find the optimum number of image sets along with their respective sub-solar point required to have a uniform distribution of pixels over a given phase range.

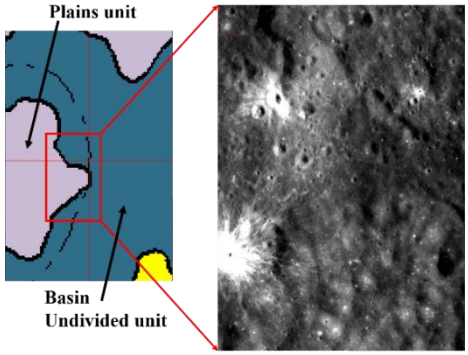

Fig 1: Figure showing the USGS geological map around Apollo 16 landing site (left) and corresponding TMC-1 image (right).

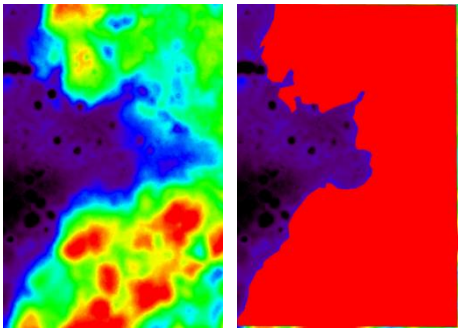

Fig 2: DEM image around Apollo 16 site provided with TMC-1 dataset showing two distinct geological units based on elevation differences (left) and marked Basin Undivided Unit in red (right).

Around 12 image sets with their respective sub solar point as shown in Table 1 were found to be optimum. Dense sampling is required at lower phase angles in order to understand opposition effect. However, it is not recommended in our case due to saturation that may occur in TMC images at lower phase angles. Table 1 also shows the sun incidence and zenith angle created at the center of the selected region. Fig. 3 shows the phase angle coverage for the whole selected region whereas

Fig. 4 shows the phase angle coverage over uniform geological area of Basin Undivided Unit.

Table 1: Description of 12 image sets with sub solar point required for nearly uniform phase angle coverage.

Sr. no.	Sub solar Point		Sun zenith (deg)	Sun Azimuth (deg)
	Latitude (ºE)	Longitude (ºN)		
1	-54.245	0	70	273.3
2	-33.905	0	50	277.6
3	-13.249	0	30	285.9
4	-2.450	0	20	295.7
5	15.496	0	09	360.0
6	33.443	0	20	64.3
7	44.242	0	30	74.1
8	54.642	0	40	79.2
9	64.898	0	50	82.4
10	75.086	0	60	84.8
11	85.238	0	70	86.7
12	95.371	0	80	88.4

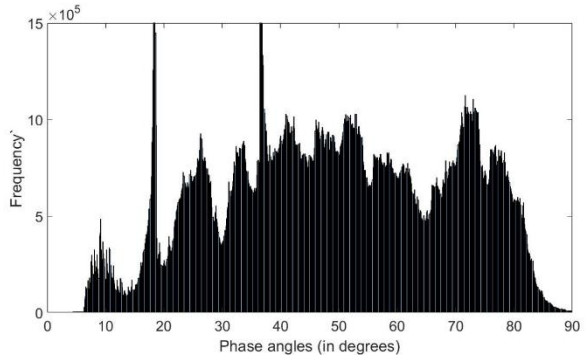

Fig 3: Figure showing the phase angle coverage (using aforementioned 12 image sets with given sub solar point) over whole selected site as shown in Fig 1.

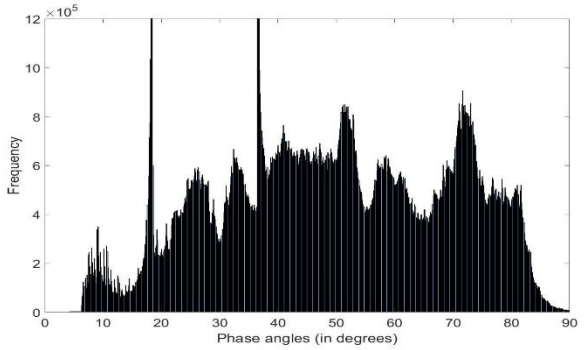

Fig 4: Figure showing the phase angle coverage (using aforementioned 12 image sets with given sub solar point) over geologically uniform area in the selected site as shown in Fig 2.

Study over sample TMC-2 image: TMC-2 image acquired on 15-10-2019 was considered. Similar datasets of count images for all three views along with ortho-rectified Nadir image, DEM image and files containing latitude-longitude and sun parameters information were present. Region around Dorsa-Geikie was selected. Using ancillary information and mathematical formulations, topographically corrected incidence and viewing angles' images were generated over the selected region. Subsequently phase angle images were generated for all three views. Despite significant differences in incidence and viewing geometry for all three views, the sun-sensor geometry was such that the phase angles were found to be in the same range over the selected site. Radiance images were also generated from count images and I/F was generated using solar irradiance values for TMC-2. Variation of LS corrected radiance factor was than observed with phase angles assuming material to have similar properties (Fig. 5).

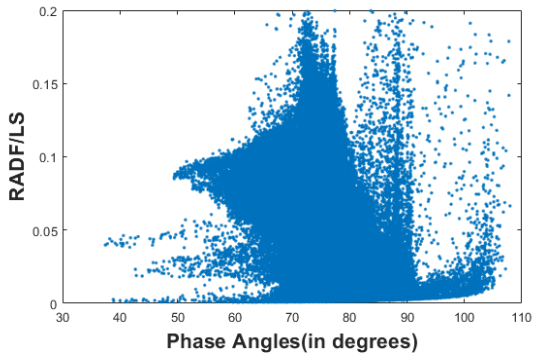

Fig 5: Figure showing the variation of LS corrected radiance factor with respect to phase angles for part of Dorsa Geikie region imaged by TMC-2 (15-10-2019).

Future prospects: With the acquisition of aforementioned sets of TMC-2 images at the required sub-solar points over Apollo 16 landing site, variation of LS corrected radiance factor can be studied with respect to a large phase angle range. Subsequently, photometric parameters may be retrieved by fitting Hapke's model which in turn can be compared with lab studies. Similar exercise can be carried out over other regions on Lunar surface subjected to availability of data.

References: [1] Hapke B. (1981) J. Geophys. Res., 86(B4), 3039-3054. [2] Hapke B. et al. (1993) Science, 260(5107), 509-511. [3] Sato H. (2014) J. Geophys. Res. Planets, 119, 1775-1805. [4] Chowdhury A. R. (2020) Curr. Sci., 118(4), 566-572. [5] Fortezzo et al. (2020) 51st LPSC, Abstract # 2760.